HSF4 Transcriptionally Activates Autophagy by Regulating ATG9a During Lens Terminal Differentiation

Jing Zhang,[1] Ning Jiang,[1] Chunxiao Du,[1,2] Hongzan Guo,[1] Ranqi Meng,[1] Xinyu Hou,[1] Mugen Liu,[3] Yanzhong Hu,[1] and Xiukun Cui[1]

[1]Joint National Laboratory for Antibody Drug Engineering, The First Affiliated Hospital, School of Medicine, Henan University, Kaifeng, China
[2]Beijing Institute of Basic Medical Sciences, Beijing, China
[3]College of Life Science and Technology, Huazhong University of Science and Technology, Wuhan, China

Correspondence: Xiukun Cui and Yanzhong Hu, Joint National Laboratory for Antibody Drug Engineering, Henan University School of Medicine, No. 1. Jin-Ming Road, Kaifeng, China; xkcui@henu.edu.cn, hyz@henu.edu.cn.

JZ, NJ, and CD contributed equally to this work.

Received: March 27, 2023
Accepted: May 16, 2023
Published: June 2, 2023

Citation: Zhang J, Jiang N, Du C, et al. HSF4 transcriptionally activates autophagy by regulating ATG9a during lens terminal differentiation. *Invest Ophthalmol Vis Sci.* 2023;64(7):5. https://doi.org/10.1167/iovs.64.7.5

Purpose. HSF4 mutations are responsible for congenital cataract formation. Dysfunction of HSF4 leads to defects in lens terminal differentiation. We aimed to study the mechanism of how HSF4 promotes organelle degradation during lens differentiation.

Methods. $HSF4^{del42}$ mutant mice that developed congenital cataracts were employed. The organelle degradation and autophagic function in lens fibers were detected by immunofluorescence and Immunoblotting. Transcriptome analysis was performed to investigate the differentially expressed genes in $HSF4^{del42}$ lenses, whereas luciferase report assay and ChIP assay were used to confirm the directly transcriptional regulation of ATG9a by HSF4.

Results. $HSF4^{del42}$ mice displayed delayed organelle clearance and impaired autophagic degradation function in lens fibers. Activation of autophagy by rapamycin ameliorated the defects in organelle clearance in $HSF4^{del42}$ lenses ex vivo and in vivo. Depletion of HSF4 attenuated autophagic flux by disrupting autophagosome biogenesis and maturation in lens epithelial cells. HSF4 directly transcriptionally activated the core autophagy protein ATG9a. Instead of the canonical ATG9a isoform, the ATG9a-X2 isoform was predominantly expressed in the lens and alleviated autophagic defects in HSF4 KO lens epithelial cells. The ATG9a-X2 protein displayed a short half-life, and rapamycin treatment restored its levels in HSF4 KO lens epithelial cells and $HSF4^{del42}$ lenses.

Conclusions. Our findings demonstrate that HSF4 facilitates organelle degradation probably by transcriptionally activating autophagy during lens terminal differentiation. We first report the involvement of HSF4 in autophagy and the tissue specific splicing of *ATG9a*. Our study indicates that autophagy activation is a possible therapeutic strategy for HSF4-related congenital cataracts.

Keywords: HSF4, lens differentiation, autophagy, ATG9a, rapamycin, organelle degradation

The ocular lens is an avascular and transparent organ that can focus light onto the retina to enable accurate vision. During embryogenesis, the anterior part of the polarized lens vesicle forms the epithelium and the posterior part differentiates into primary fibers.[1,2] Lens growth occurs throughout an organism's lifetime concomitantly with continuous cellular differentiation events in which epithelial cells at the equator of the lens withdraw from the cell cycle and differentiate into secondary fiber cells.[3,4] To achieve transparency, fiber cells in the core of the lens undergo terminal differentiation, which is characterized by the clearance of nuclei and organelles (forming the organelle-free zone [OFZ]) and robust expression of lens crystallins.[5,6] Defects in the removal of nuclei or organelles in lens fibers cause congenital cataracts.[7] For instance, knockout of lens-specific DNase in mice (DNase IIβ) and zebrafish (DNase 1l1l) abrogates the denucleation process and causes cataracts.[8,9] However, the detailed molecular mechanism of lens organelle degradation is still being elucidated.

Autophagy is a conserved lysosomal degradation pathway that maintains cell homeostasis via removal and recycling of needless cellular contents, such as damaged organelles.[10,11] Autophagy can be divided into macroautophagy, microautophagy, and chaperone-mediated autophagy, among which macroautophagy (hereafter referred to as *autophagy*) has been extensively studied. Defects in autophagy related genes are associated with congenital cataract formation. Mutations in human FYCO1, an autophagy receptor for autophagosome transport by linking LC3, are responsible for autosomal recessive congenital cataracts.[12–14] EPG5 is an RAB7 effector and is specifically required for fusion between autophagosomes and lysosomes during autophagy.[15] Homozygous mutations of EPG5 are associated with Vici syndrome, which is

characterized by congenital cataracts and other neurodevelopmental symptoms.[16,17] Rab3GAP1, Rab3GAP2 and TBC1D20 mutations cause Warburg micro syndrome, whose clinical features include congenital cataracts, and brain and endocrine abnormalities.[18–20] Studies have indicated that Rab3GAP1, Rab3GAP2, and TBC1D20 are involved in autophagosome biogenesis and maturation.[21–23] However, it is unclear how the aberrant autophagy induced by gene mutations leads to congenital cataracts.

Although evidence suggests that autophagy participates in embryogenesis and numerous tissue differentiation processes, the role of autophagy in lens fiber terminal differentiation is controversial. ATG5 and VPS34 lens-specific knockout mice have normal degradation of organelles in lens fiber cells, although Atg5-deficient mice develop age-related cataracts and VPS34-deficient mice develop congenital cataracts.[24,25] However, constitutively activated autophagy can indeed be observed in the lens epithelium and fibers during lens differentiation. Autophagic vesicles containing organelles (e.g., mitochondria) exist in human lens epithelial cells and differentiating fiber cells.[26] Autophagy structures are present in chick embryo lenses, and mitophagy can be induced by serum starvation in chicken primary lens cells.[26] Experiments using transgenic mouse models have suggested that pronounced autophagy occurs in embryonic and adult lenses, whereas only a low degree of mitophagy is observed.[27] Both inactivation of mechanistic target of rapamycin (mTOR) by rapamycin exposure and suppression of PI3K signaling can induce autophagy and premature loss of organelles in chicken embryo lens fibers.[28,29] Moreover, autophagy activated by rapamycin treatment alleviates the organelle degradation defects and the cataract phenotype in *gja8b* mutant zebrafish lenses.[30] Deletion of the mitophagy receptor BNIP3L/NIX in mice leads to retention of mitochondria, endoplasmic reticulum and Golgi apparatus in differentiating lens fiber cells.[31] Deficiency in *Tdrd7*, a gene responsible for congenital cataract, disrupts autophagic flux and maturation of autophagosomes and then causes failure to clear of organelles during the lens fiber differentiation process in mice.[22,32] Dysfunction of FYCO1 in mice leads to impaired autophagic flux, defects in organelle degradation of lens fibers and cataract formation.[13] These data suggest that autophagy is indispensable during lens differentiation and that its intricate role needs to be further investigated.

HSF4, a member of the heat shock factor family, is specifically expressed in the ocular lens.[33,34] Mutations in human HSF4 cause autosomal dominant and recessive congenital cataracts.[35–37] Both HSF4-deficient mice and zebrafish develop congenital cataracts and display lens differentiation defects including failures in degrading nuclei and organelles of lens fiber cells.[34,38–40] Our previous studies have suggested that HSF4 transcriptionally activates lens-specific DNase to promote nuclear DNA degradation during lens de-nucleation process.[9,41] However, the molecular mechanism by which HSF4 promotes the clearance of organelles during lens fiber differentiation is unknown. In the present study, we found that both organelle clearance and autophagic degradation function were impaired in lens fibers of HSF4^{del42} mice. Rapamycin treatment ameliorated organelle degradation defects in the HSF4^{del42} lens ex vivo and in vivo. Deficiency in HSF4 attenuated autophagic flux by disrupting autophagosome initiation and maturation in lens epithelial cells. HSF4 transcriptionally regulated the expression of ATG9a, which was highly expressed in differentiating lens fibers. Rapamycin treatment restored the levels of the lens-dominant ATG9a isoform ATG9a-X2. Our data demonstrate that HSF4 transcriptionally activates autophagy by regulating lens-dominant ATG9a isoform during lens differentiation.

Materials and Methods

Animals

Wild-type (WT) and HSF4^{del42} C57/BL6 mice were fed and bred in an SPF-grade animal room as described in our previous study.[42] The HSF4^{del42} mice were generated by the CRISPR-Cas9 technology which gRNAs targeted the exon 5 of *Hsf4*. A 42-amino acid (121-163 aa) in-frame deletion was introduced into HSF4 protein and disrupted its transcription activities. All animal experiments in this study were approved by the Ethics Committee of Henan University School of Medicine. For lens culture ex vitro, p3 mice were euthanized, and then the lenses were isolated carefully and cultured in complete M199 medium (12350039; Thermo Fisher Scientific, Waltham, MA, USA) with 20% fetal bovine serum at 37°C. The cultured lenses were incubated with 10 µM rapamycin (S1039; Selleck Chemicals, Houston, TX, USA) for 12 hours. For intraperitoneal administration, p3 mice were anesthetized with isoflurane and injected with 7.5 mg/kg rapamycin (dissolved in 2% DMSO, 30% PEG300, and 5% Tween 80) using 29 G insulin syringes (U-40; BD Bioscience, Franklin Lakes, NJ, USA). Forty-eight hours later, the mice were euthanized, and the lenses were dissected for further analysis.

Cell Lines, Plasmids, Antibodies, and Reagents

The mouse lens epithelial cell lines and HEK293T cells were cultured in DMEM (11965092; Thermo Fisher Scientific) containing 10% FBS and 1 × streptomycin and penicillin (15070063; Thermo Fisher Scientific) in 37°C incubators with 5% CO_2. The WT mouse lens epithelial cell line was generated from p2 lens epithelial cells of C57/BL6 mice and immortalized by SV40. The HSF4 knockout cell lines were constructed by CRISPR-Cas9 technology from the WT lens cell line as described in our previous study.[42] The full-length STX17 and ATG9a CDSs were cloned from mouse lens cDNA and separately inserted into the pmcherry-C1 vector and 3 × Flag CMV 7.1 vectors. ATG9a (67096-1-Ig), HSF4 (18797-1-AP), ATG3 (11262-2-AP), and GRP78 (11587-1-AP) antibodies were purchased from Proteintech Group (Rosemont, IL, USA), whereas p62 (ab109012), WIPI2 (ab105459), Tomm20 (ab186735), and KDEL (ab176333) antibodies were purchased from Abcam plc (Cambridge, MA, USA). Antibodies against lamin A/C (4777), Gabarapl1 (6632), HA-tag (3724) and β-actin (3700) were obtained from Cell Signaling Technology (Danvers, MA, USA). An LC3 antibody (NB100-2220) was purchased from Novus Biologicals (Littleton, CO, USA), and a GM130 antibody (610822) was purchased from BD Biosciences. Rapamycin (S1039), MG132 (S2619) and Baf-A1 (S1413) were purchased from Selleck Chemicals, and chloroquine (50-63-5) was purchased from Sigma-Aldrich (St. Louis, MO, USA). The mTOR siRNAs (siG161206075457-1-5 and siG161206075517-1-5) were ordered from Guangzhou RiboBio company (Guangzhou, China).

Histology and Immunofluorescence

For paraffin sections, eyes from WT and HSF4^{del42} mice were fixed in 4% PFA overnight at 4°C and then embedded in paraffin. The lenses were sliced into 2 µm slices with a microtome (Leica Biosystems, Wetzlar, Germany). After antigen retrieval, the slices were blocked with 1% goat serum for two hours and incubated with primary antibodies overnight at 4°C. After being washed with TBST buffer (0.1% Triton X-100 in TBS), the slices were incubated with Alexa Fluor 488/594-conjugated secondary antibodies (A-11001 and A-11005; Thermo Fisher Scientific) for one hour at room temperature. Then, the sections were washed with TBST buffer, and the nuclear DNA was stained with DAPI dye (D9542; Sigma-Aldrich). The images were captured with a confocal laser-scanning microscope (Nikon Precision, A1R; Nikon Inc., Melville, NY, USA).

Immunoblotting, RNA-Sequence, and qRT–PCR

The immunoblotting and qRT–PCR procedures were described in our previous study.[42] Lysates of lens tissues and cell lines were prepared with 1 × SDS buffer (62.5 mM Tris-HCl, pH 6.8, 2% SDS, 10% glycerol) with a protease inhibitor cocktail (A32961; Thermo Fisher Scientific). Equal amounts of total protein were subjected to SDS–PAGE analysis and transferred to PVDF membranes. After incubation with the primary and HRP-conjugated secondary antibodies, the signals were developed with ECL substrates (34580; Thermo Fisher Scientific) and detected with a chemiluminescence imaging system (Tanon Biology, Shanghai, China). Densitometry of immunoblotting bands was measured by Quantity One software.

For RNA-sequence, next-generation sequencing and data analysis were performed by GENEWIZ (Suzhou, China) using Illumina NovaSeq platform. For qRT–PCR, 2 µg of total RNA was used to synthesize cDNA, which was mixed with SYBR Green PCR Master Mix (Applied Biosystems, A46111) and amplified in an ABI 7500 Fast System. The primers for mouse ATG9a were as follows: forward, 5′ggatttacctgtatgctgctgggagaa3′ and reverse, 5′cgcatcggggagagtaactttcaag3′. Student's *t* test was used for statistical analysis, and * represents $P < 0.01$.

Luciferase Reporter Assay and Chromatin Immunoprecipitation Assay

The promoter of mouse ATG9a (from −2632 to −7) was obtained from mouse lens genomic DNA and inserted into pGL3-basic vectors. Then, HEK293T cells were cotransfected with mATG9 promoter luciferase reporters, flag-HSF4, and pRL-TK Renilla vectors for 36 hours. The cell lysates were prepared with passive lysis buffer, and luciferase activities were determined with a Dual-Luciferase Assay system (E1910; Promega Biotech, Finnboda Varvsväg, Sweden) following standard protocols. Renilla luciferase activity was used as the control.

The ChIP assay was performed following the standard protocol of chromatin immunoprecipitation kits (17–295; Upstate Biotechnology, Charlottesville, VA, USA). Briefly, 5×10^6 cells were fixed with 1% PFA for 10 minutes at 37°C to cross-link the protein–DNA complex. The cells were lysed with SDS buffer, and the genomic DNA was broken into 200 to 2000 bp fragments by ultrasonication. After incubation with an anti-HA antibody overnight at 4°C, the protein-DNA complex was precipitated with protein A agarose plus salmon sperm DNA and then dissociated at 65°C for four hours. The DNA was purified with the phenol-chloroform extraction method and used for qRT–PCR. The primers for the predicted HSEs of mATG9a were as follows: HSE1-forward, 5′ aggggcaggggaggaaacttt 3′ and HSE1-reverse, 5′ ccaggccagagggaatgagaaa 3′; HSE2-forward, 5′ aggcacccagggaacccacttat 3′ and HSE2-reverse, 5′ acccagtgcagagtgagtcagtacag 3′; HSE3-forward, 5′ gcgggtgacagtgaatgacagacg 3′ and HSE3-reverse, 5′ cgcgcgccctctatcaaaacat 3′; HSE4-forward, 5′ cccgctcccacaaatcagttctg 3′ and HSE4-reverse, 5′ gccgccgaattgttgtggtgtt 3′.

Statistical Analysis

Statistical analysis was performed with SPSS 13.0 and GraphPad Prism 8 software. Differences were statistically analyzed using Student's *t* test.

Results

HSF4^{del42} Mice Displayed Defective Organelle Clearance in Lens Fibers

In our previous study, an HSF4-mutated mouse line (HSF4^{del42}) was generated using CRISPR-Cas9 technology.[42] The HSF4^{del42} mice harbored a 42-aa deletion of the HSF4 protein, which disrupted its transcriptional activity, and developed congenital cataracts (Figs. 1A, 1B). To determine organelles degradation in HSF4^{del42} lenses, the amounts of nuclei, mitochondria, endoplasmic reticulum (ER), and Golgi apparatus were first detected in p7 WT and HSF4^{del42} mouse lens fibers with immunoblotting. Our data showed that the levels of the organelle protein markers lamin A/C, Tomm20, GRP78, and GM130 were obviously elevated in HSF4^{del42} lens fibers compared with those in WT lens fibers (Fig. 1C). Then immunofluorescence was performed to confirm organelle degradation in p7 WT and HSF4^{del42} lenses. Our results indicated that the fluorescence signals of lamin A/C, Tomm20, KDEL, and GM130 were restricted to superficial cortical fibers in WT lenses. In contrast, lamin A/C, Tomm20, KDEL, and GM130 signals could be observed in both cortical and central fibers in HSF4^{del42} lenses (Figs. 1D–F). These data suggested that the clearance of nuclei and membrane-bound organelles was disturbed in HSF4^{del42} mouse lens fibers.

HSF4^{del42} Lens Fibers had Impaired Autophagic Degradation Function

To determine whether autophagic function was impaired in HSF4-deficient lenses. Autophagic function was first assessed in p7 WT and HSF4^{del42} lenses using immunofluorescence with antibodies against the autophagy markers LC3 and SQSTM1/p62. Our data showed that p62-positive puncta were present from cortical fibers to central fibers in HSF4^{del42} lenses, while they were observed only in superficial cortical fibers in WT lenses (Fig. 2A). Similar data were obtained for LC3-positive puncta in both cortical and central fibers in HSF4^{del42} lenses compared with WT lenses (Fig. 2B). To further confirm the autophagic function, the protein levels of LC3 and p62 were determined in WT and HSF4^{del42} mouse lenses with immunoblotting. Consistent with the immunofluorescence data, we found that the levels of lipidated LC3-II and p62 were significantly higher in HSF4^{del42} lenses than in WT lenses (Figs. 2C–E). Moreover, both LC3-II and p62 levels

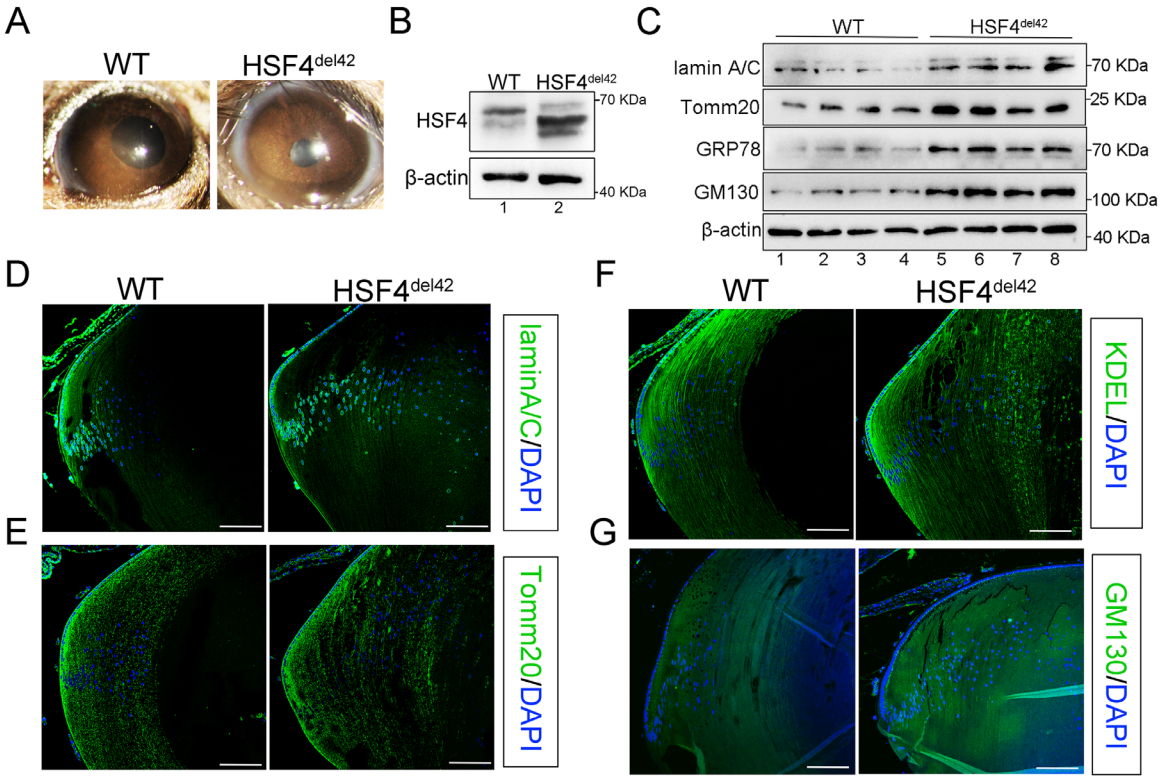

Figure 1. HSF4^{del42} mice displayed impaired organelle clearance in lens fibers. (**A**) HSF4^{del42} mice developed congenital cataracts. (**B**) HSF4 protein was detected in p7 WT and HSF4^{del42} lens fibers. (**C**) Organelle markers were detected by western blotting in p7 WT and HSF4^{del42} lens fibers. β-actin was used as the control. (**D–G**) Organelles were detected by immunofluorescence in p7 WT and HSF4^{del42} lens fibers. The nuclei were stained with DAPI. Bar, 100 µm. The nuclear envelope was labeled with lamin A/C. The mitochondria were labeled with Tomm20. The endoplasmic reticulum was labeled with GRP78 or KDEL, and the Golgi apparatus was labeled with GM130.

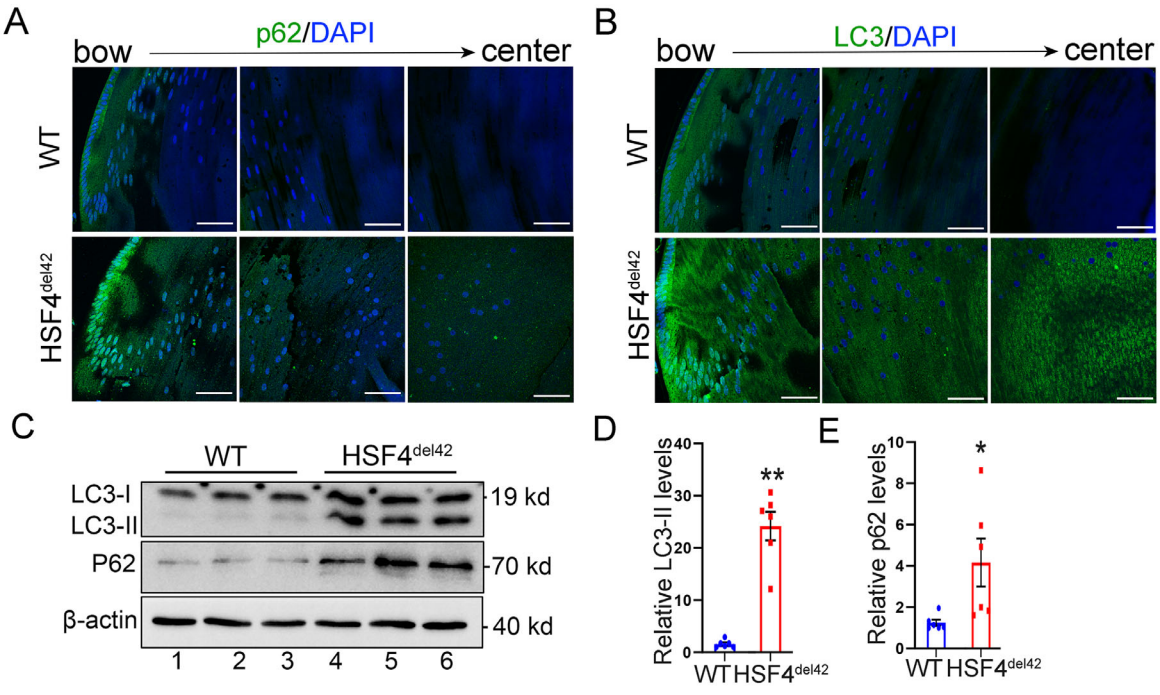

Figure 2. HSF4^{del42} mice had autophagic degradation defects in lens fibers. (**A, B**) p62 and LC3 signals were detected by immunofluorescence from cortical fibers to central fibers in p7 WT and HSF4^{del42} lenses. The nuclei were stained with DAPI. Bar, 50 µm. (**C**) Levels of LC3-II and p62 were detected by western blotting in WT and HSF4^{del42} lenses. β-actin was used as the control. Student's t test was used for statistical analysis. n = 6, $^{*}P < 0.05$, $^{**}P < 0.01$.

Investigative Ophthalmology & Visual Science

were obviously increased in HSF4^{del42} lens fibers (Supplementary Fig. S1). The levels of polyubiquitinated proteins were also detected in WT and HSF4^{del42} lens fibers. Our results suggested that depletion of HSF4 led to accumulation of ubiquitinated protein in mouse lens fibers (Supplementary Fig. S2). These data suggested an impaired autophagic degradation function in HSF4^{del42} lenses.

Rapamycin Treatment Ameliorated Lens Organelle Degradation Defects in HSF4^{del42} Mice Ex Vivo and In Vivo

Given that both organelle clearance and autophagic degradation function were impaired, we wondered whether the failure of organelle clearance in HSF4^{del42} lens fibers was due to defective autophagic degradation. To address this issue, autophagy was induced by exogenous stimuli (e.g., rapamycin), and the organelle clearance in HSF4^{del42} lenses was detected. The p3 WT and HSF4^{del42} lenses were dissected carefully and cultured ex vivo for 24 hours. The lenses in ex vivo models were treated with 10 µM rapamycin for 12 hours to induce autophagy and subjected to immunoblotting. The elevated LC3-II levels and decreased p62 levels demonstrated an obvious induction of autophagy in WT and HSF4^{del42} lenses treated with rapamycin (Fig. 3A). Although rapamycin treatment did not alter the levels of the membrane-bound organelle markers GM130, GRP78, and Tomm20 in WT lenses, it indeed reduced the GM130, GRP78, and Tomm20 levels in HSF4^{del42} lenses (Fig. 3A). Unexpectedly, the nuclear envelope component lamin A/C

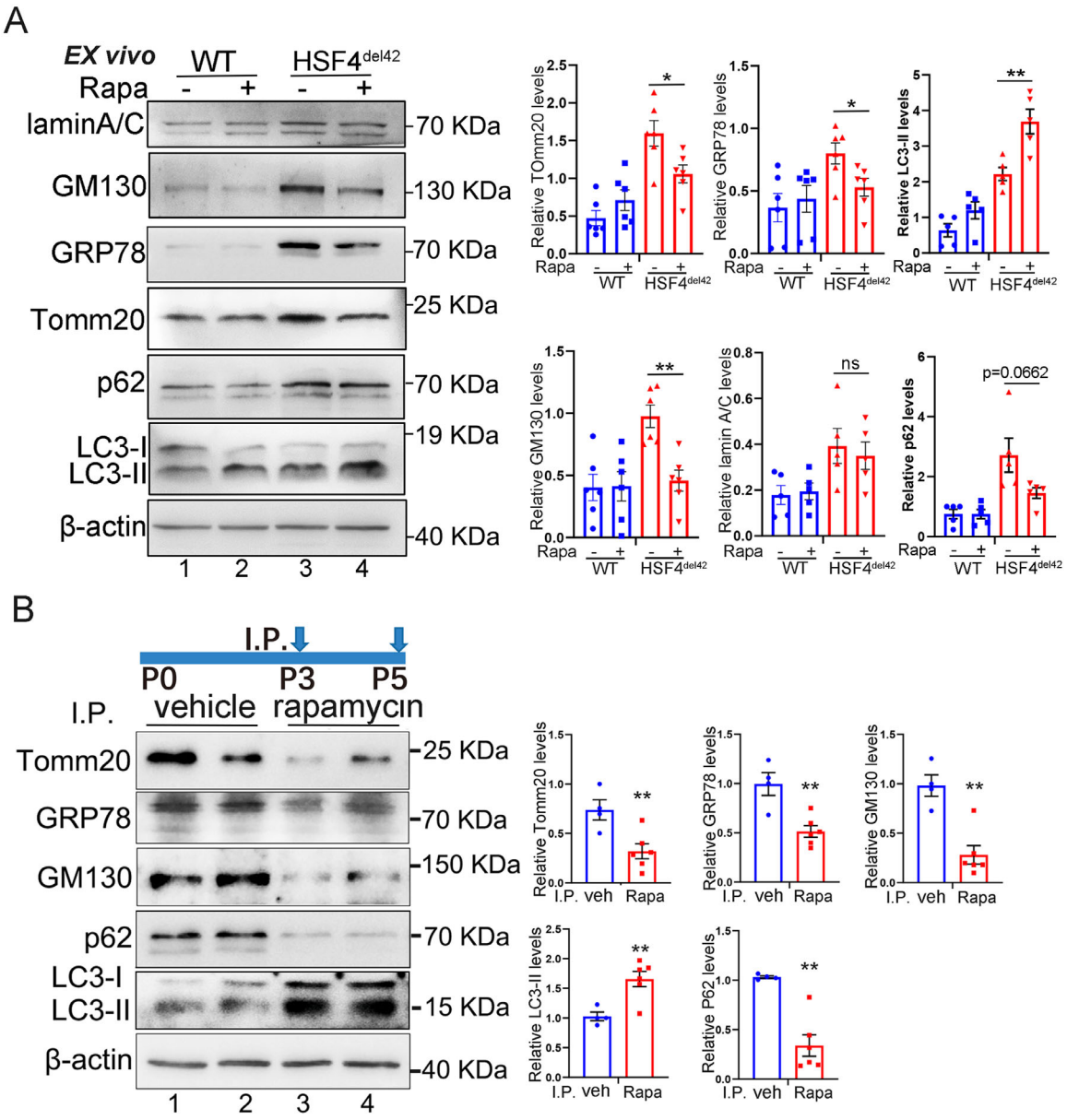

Figure 3. Activation of autophagy by rapamycin promoted organelle degradation in HSF4^{del42} lenses. (**A**) The p3 WT and HSF4^{del42} lenses were cultured and treated with 10 µM rapamycin for 12 hours ex vivo. The levels of organelle markers were detected by Western blotting. Student's *t* test was used for statistical analysis. n = 6, $^{*}P < 0.05$, $^{**}P < 0.01$. ns, no significance. (**B**) The p3 HSF4^{del42} mice were injected intraperitoneally (I.P.) with 7.5 mg/kg rapamycin or vehicle for 48 hours. Organelle markers in lens fibers were detected by western blotting. Student's *t*-test was used for statistical analysis. rapamycin (n = 6) and vehicle (n = 4). $^{**}P < 0.01$.

levels were not changed in either WT or HSF4^{del42} lenses when treated with rapamycin (Fig. 3A). Then, we assessed the effect of rapamycin treatment on organelle degradation in HSF4^{del42} lens in vivo. Newborn HSF4^{del42} mice were injected intraperitoneally (I.P.) with 7.5 mg/kg rapamycin at p3, and then the lenses were dissected carefully for further analysis at p5. Our immunoblotting results indicated that I.P. administration of rapamycin efficiently increased LC3-II levels and reduced p62 levels in HSF4^{del42} lens fibers as a consequence of autophagy induction (Fig. 3B). Intraperitoneal injection of rapamycin caused sharp declines in GM130, GRP78, and Tomm20 protein levels in the lens fibers of HSF4^{del42} mice compared with those of vehicle-injected mice (Fig. 3B). These observations supported the idea that autophagy induction by rapamycin facilitated the degradation of detained membrane-bound organelles, such as mitochondria, endoplasmic reticulum, and Golgi apparatus, in HSF4^{del42} lens fibers.

Depletion of HSF4 Attenuated Autophagic Flux by Disrupting Autophagosome Biogenesis and Maturation

The defects in autophagic degradation function could have been a result of the disturbance in autophagic flux, impaired lysosomal activity, or both. Although our previous study showed that HSF4 is involved in the maintenance of lysosomal acid pH,[43] we focused on its function in autophagic flux in this study. To confirm the roles of HSF4 in autophagic flux, the LC3 and p62 levels were assessed in WT and three HSF4-knockout mouse lens epithelial cell lines[42] (referred to as mLEC, #1, #2, and #3, respectively) that were treated with 20 µM chloroquine to inhibit autolysosome activities. The immunoblotting data indicated that knockout of HSF4 significantly reduced LC3-II levels and increased p62 levels in lens epithelial cells (Figs. 4A–C). The LC3-II and p62 levels were obviously elevated under chloroquine treatment in WT mLECs, whereas they increased less in HSF4 knockout #3 (referred to as *HSF4 KO*) mLECs (Figs. 4A–C). These data suggested a weaker autophagic flux in HSF4 KO mLECs than in WT mLECs. Then, autophagic flux was monitored by mRFP-EGFP-LC3 assay in WT and HSF4 KO mLECs treated with rapamycin. An abundance of LC3 puncta, including all GFP-positive (GFP+) and RFP-positive (RFP$^+$) puncta, accumulated in WT mLECs, while there were only sparse enlarged LC3 puncta in HSF4 KO mLECs (Figs. 4D, 4E). Moreover, the percentage of GFP$^-$RFP$^+$ LC3 puncta in HSF4 KO mLECs was significantly lower than that in WT mLECs (Figs. 4D, 4F). Mature autophagosomes fuse with lysosomes to form autolysosomes that degrade cargos. Thus, the

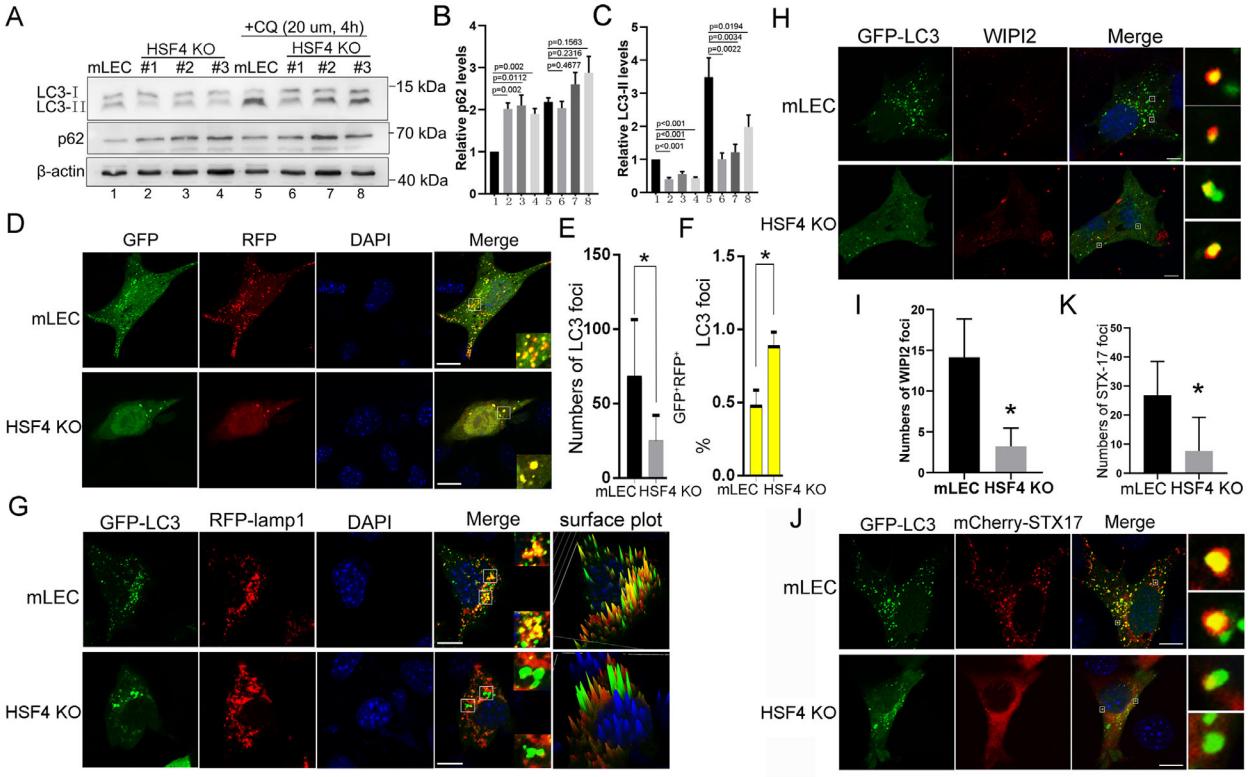

Figure 4. HSF4 maintained autophagic flux by facilitating autophagosome biogenesis and maturation. (**A–C**) The levels of LC3-II and p62 were detected and analyzed in WT and three HSF4 knockout mLEC stable lines (referred to as HSF4 KO) treated with/without 20 µM chloroquine (CQ) for four hours. The β-actin was used as the control. Student's *t* test was used for statistical analysis. (**D**) GFP and RFP signals were observed in WT and HSF4 knockout mLEC lines transfected with GFP-RFP-LC3 vectors. The nuclei were stained with DAPI. Bar, 10 µm. (**E, F**) The numbers of total LC3 foci and GFP$^+$RFP$^+$ foci in (**D**) were counted. Student's *t* test was used for statistical analysis. n = 15, $^*P < 0.05$. (**G**) The colocalization between GFP-LC3 and lysosomes (labeled with RFP-lamp1) was detected in WT and HSF4 knockout mLEC lines. The nuclei were stained with DAPI. *Bar:* 10 µm. (**H**) The biogenesis of autophagosomes was indicated with WIPI2 in WT and HSF4-knockout mLECs. The nuclei were stained with DAPI. *Bar:* 10 µm. (**I**) The numbers of WIPI2 foci in (**H**) were counted. Student's *t* test was used for statistical analysis. n = 10, $^*P < 0.05$. (**J**) The maturation of autophagosomes was indicated with GFP-LC3 and mCherry-STX17 in WT and HSF4 knockout mLECs. The nuclei were stained with DAPI. *Bar:* 10 µm. (**K**) The numbers of LC3-positive STX17 foci in (**J**) were counted. Student's *t* test was used for statistical analysis. n = 15, $^*P < 0.05$.

Investigative Ophthalmology & Visual Science

colocalization between autophagic vacuoles and lysosomes was determined in WT and HSF4 KO mLECs that expressed GFP-LC3 and RFP-lamp1. In WT mLECs, numerous colocalizations between LC3 puncta and lysosomes existed. In contrast, the enlarged LC3 puncta hardly overlapped with lysosomes in HSF4 KO mLECs (Fig. 4G). These data suggested that HSF4 deficiency resulted in defective autophagic flux in lens epithelial cells.

The failure of autolysosome formation could have been induced by defects in autophagosome maturation or autophagosome fusion. As shown in Figure 4D, there were sharp declines in LC3 puncta numbers and abnormally enlarged LC3 puncta in HSF4 KO mLECs. We speculated that knockout of HSF4 may have impaired the autophagosome formation process. To further characterize the steps at which autophagy was blocked, autophagy factors essential for autophagosome biogenesis and maturation were analyzed in WT and HSF4 KO mLECs. WIPI2, which exists on the phagophore but not on mature autophagosomes, is considered to be a marker of autophagosome initiation.[44] Our results indicated that the accumulation of WIPI2 puncta was obviously decreased in HSF4 KO mLECs compared with WT mLECs. The colocalization between the LC3 foci and WIPI2 puncta was also reduced in HSF4 KO mLECs (Figs. 4H, 4I). To assess the maturation of autophagosomes, mCherry-STX17, a complete autophagosome marker,[45] was expressed in WT and HSF4 KO mLECs. Robust accumulation of LC3-positive STX17 puncta was observed in WT mLECs under rapamycin treatment. In contrast, diffuse STX17 signals with few puncta were observed in HSF4 KO mLECs (Figs. 4J, 4K). These data suggested that HSF4 deficiency resulted in aberrant autophagosome initiation and maturation. In summary, these data demonstrated that HSF4 maintained autophagic flux by promoting autophagosome biogenesis and maturation in lens epithelial cells.

HSF4 Transcriptionally Regulated ATG9a Expression

To ascertain the molecular mechanism by which HSF4 transcriptionally regulates autophagy, transcriptomes were sequenced in p3 and p7 WT and HSF4^{del42} mouse lens fibers. In total, 82 upregulated and 417 downregulated genes were identified in both p3 and p7 HSF4^{del42} lens fibers (Fig. 5A). KEGG pathway and Gene Ontology analysis indicated that the genes with altered expression contained a pack of autophagy related genes, among which ATG3, ATG9a, and Gabarapl1 are core autophagy factors (Figs. 5B, 5C). Immunoblotting data showed that the ATG9a protein levels were markedly decreased in HSF4^{del42} lens fibers (Figs. 5D, 5E). In contrast, the protein levels of Gabarapl1 were moderately decreased while the ATG3 protein levels remained unchanged in HSF4^{del42} lens fibers (Figs. 5D, 5F, 5G). The significant decrease of ATG9a mRNA levels were further verified in WT and HSF4^{del42} lens fibers (Figs. 5H). ATG9a is the sole integral membrane protein of core autophagy-related genes and is required for both initiation and expansion of the autophagosome.[46] Accordingly, we focused on ATG9a in our following studies. Moreover, both the ATG9a mRNA and protein levels were reduced in all three HSF4-knockout mLEC cell lines compared with WT mLECs (Supplementary Fig. S3). To confirm whether HSF4 directly transcribes ATG9a, ATG9a luciferase reporters containing a 2.6 kb fragment of the mouse ATG9a promoter (from –2632 to –7) were cotransfected with HSF4 vectors into HEK293T cells. Compared with that in cells transfected with empty vectors, the luciferase activity of ATG9a reporters was raised nearly sixfold in cells overexpressing HSF4 (Fig. 5I). HSF4 transcribes downstream genes via direct binding to heat shock elements (HSEs) at their promoters, and four HSEs were predicted to exist in the mouse ATG9a promoter. Because of lacking a suitable HSF4 antibody for immunoprecipitation, the binding abilities of HSF4 to these HSEs were determined by the ChIP assay using a HA-tag antibody in HSF4 KO mLECs overexpressing HA-HSF4. Our ChIP data showed that HSF4 robustly bound to HSE2 (–887 to –880 and –829 to –807), slightly bound to HSE1 (–338 to –331 and –264 to –257), but not to HSE3 (–1522 to –1515) and HSE4 (–1979 to –1967) in lens epithelial cells (Fig. 5J). These results indicated that HSF4 activated ATG9a expression through direct binding to its promoter.

To elucidate the function of ATG9a during lens fiber differentiation, the expression pattern of ATG9a was determined in p3 WT mouse lenses with immunofluorescence. The signals indicated that ATG9a was highly expressed in the central anterior epithelia (EC), equatorial epithelia (EQ) and cortical fiber (FP), and moderately expressed in the transitional zone (TZ), but not in the central fiber (FC) (Figs. 6A–E). In lens cortical fibers where organelles undergo intensive degradation, ATG9a formed puncta and colocalized with LC3-positive autophagic vesicles (Figs. 6F–Fii). Moreover, ATG9a puncta colocalized with membrane-bound organelles, such as mitochondria (Figs. 6G–Gii), the endoplasmic reticulum (Figs. 6H–Hii) and the Golgi apparatus (Figs. 6I–Iii), as well as the nuclear envelop (Supplementary Fig. S4). These data implied that ATG9a-mediated autophagy played an essential role in membrane-bound organelle clearance in differentiating lens fibers.

Rapamycin Treatment Elevated Lens-Dominant ATG9a Isoform Levels in HSF4 Deficient Lens and mLECs

Several ATG9a protein isoforms are produced by alternative splicing in mice, among which isoform a (NP_001275541.1, referred to as ATG9a-a) is the most studied. Unexpectedly, we found that the ATG9a transcript variant X3 (XM_011238689.4) was dominantly expressed in mouse lens tissue (Figs. 7A, 7B). The ATG9a transcript variant X3 skipped exon 13 and caused a frameshift from serine at the 677 sites, which produced the ATG9a protein isoform X2 (XP_011236991.1, referred to as ATG9a-X2) with a distinctive C-terminus (Fig. 7A, 7C). The ATG9a-X2 isoform formed puncta colocalized with LC3 foci in mLECs when treated with the lysosomal activity inhibitor bafilomycin A1 (Baf-A1) (Fig. 7D). Both ATG9a-a and ATG9a-X2 mRNA levels were decreased in HSF4^{del42} lens fibers (Supplementary Fig. S5). Overexpression of ATG9a-X2 partially recovered the LC3-II levels and decreased p62 levels in HSF4 KO mLECs (Fig. 7E). These data indicated that ATG9a-X2 could fulfill autophagic functions in mLECs. Compared to isoform a, ATG9a isoform X2 displayed a lower protein level and was restored by both Baf-A1 and the proteasome inhibitor MG132, which suggested a short half-life (Fig. 7F). As shown in Figure 3, rapamycin treatment alleviated the organelle degradation defect in HSF4^{del42} lenses, in which the ATG9a mRNA levels were irreversibly decreased by HSF4 deficiency. Previous studies have suggested that rapamycin treatment can restore

Investigative Ophthalmology & Visual Science

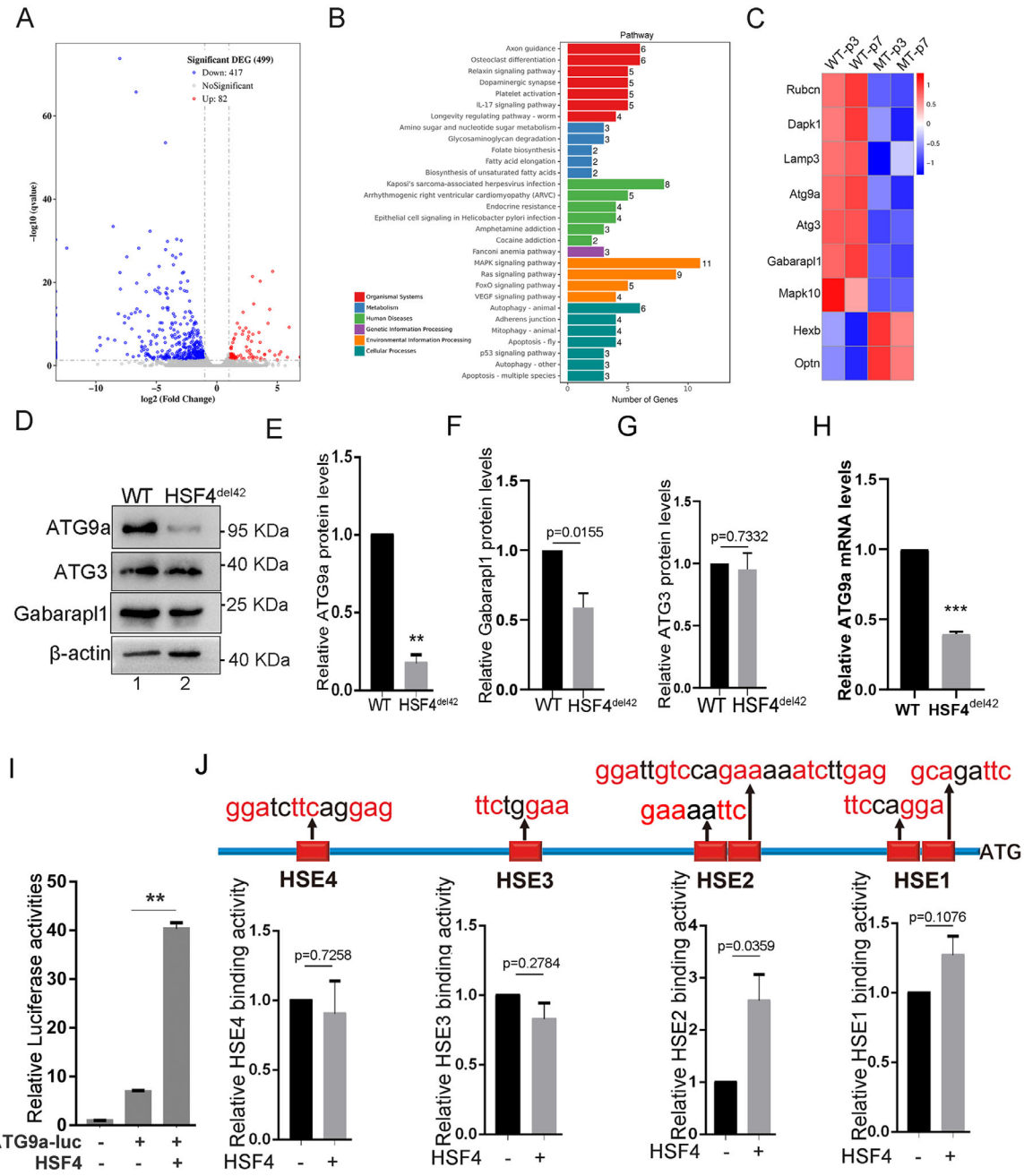

Figure 5. HSF4 transcriptionally regulated ATG9a. (**A**) The volcano plot shows the differentially expressed genes (82 upregulated and 417 downregulated) between both p3 and p7 WT and HSF4^{del42} lens fibers identified by RNA-seq. The *red* and *blue points* indicate the upregulated and downregulated genes, respectively. (**B**) Gene ontology (GO) analysis was performed to classify the differentially expressed genes between WT and HSF4^{del42} lens fibers. (**C**) Heatmap showing the differentially expressed autophagy related genes in WT and HSF4^{del42} lens fibers. (**D**) Protein levels of the core autophagy genes ATG9a, ATG3, and Gabarapl1 were verified in p7 WT and HSF4^{del42} lens fibers. The β-actin was used as the control. (**E–G**) Levels of ATG9a, ATG3, and gabarapl1 in (**E**) were statistically analyzed. Student's *t* test was used for statistical analysis. n = 3, $^{**}P < 0.01$. (**H**) The mRNA levels of ATG9a were detected by real-time PCR in WT and HSF4^{del42} lens fibers. Student's *t* test was used for statistical analysis. n = 3, $^{***}P < 0.001$. (**I**) Luciferase activities of ATG9a promoter reporters were measured in HEK293T cells overexpressing HSF4. Student's *t* test was used for statistical analysis. n = 3, $^{**}P < 0.01$. (**J**) HSEs were predicted in the ATG9a promoter and the conserved nucleotides of HSE sequence (nGAAn) were marked in *red*. The ability of HSF4 to bind to the predicted HSEs was detected by ChIP assay with a HA-tag antibody in HSF4 KO mLECs overexpressing HA-HSF4. Student's *t* test was used for statistical analysis. n = 3.

ATG9a protein levels in yeast.[47] We wondered whether rapamycin treatment could recover ATG9a-X2 protein levels in mLECs and HSF4^{del42} lenses. Our data indicated that ATG9a-X2 protein levels were increased in mLECs that were treated with rapamycin for 3 hours, 6 hours, and 12 hours (Fig. 7G). Knockdown of mTOR by siRNA also elevated the ATG9a-X2 protein levels in HSF4 KO mLECs (Fig. 7H). Moreover, ATG9a-X2 levels were also increased in p3 HSF4^{del42}

Investigative Ophthalmology & Visual Science

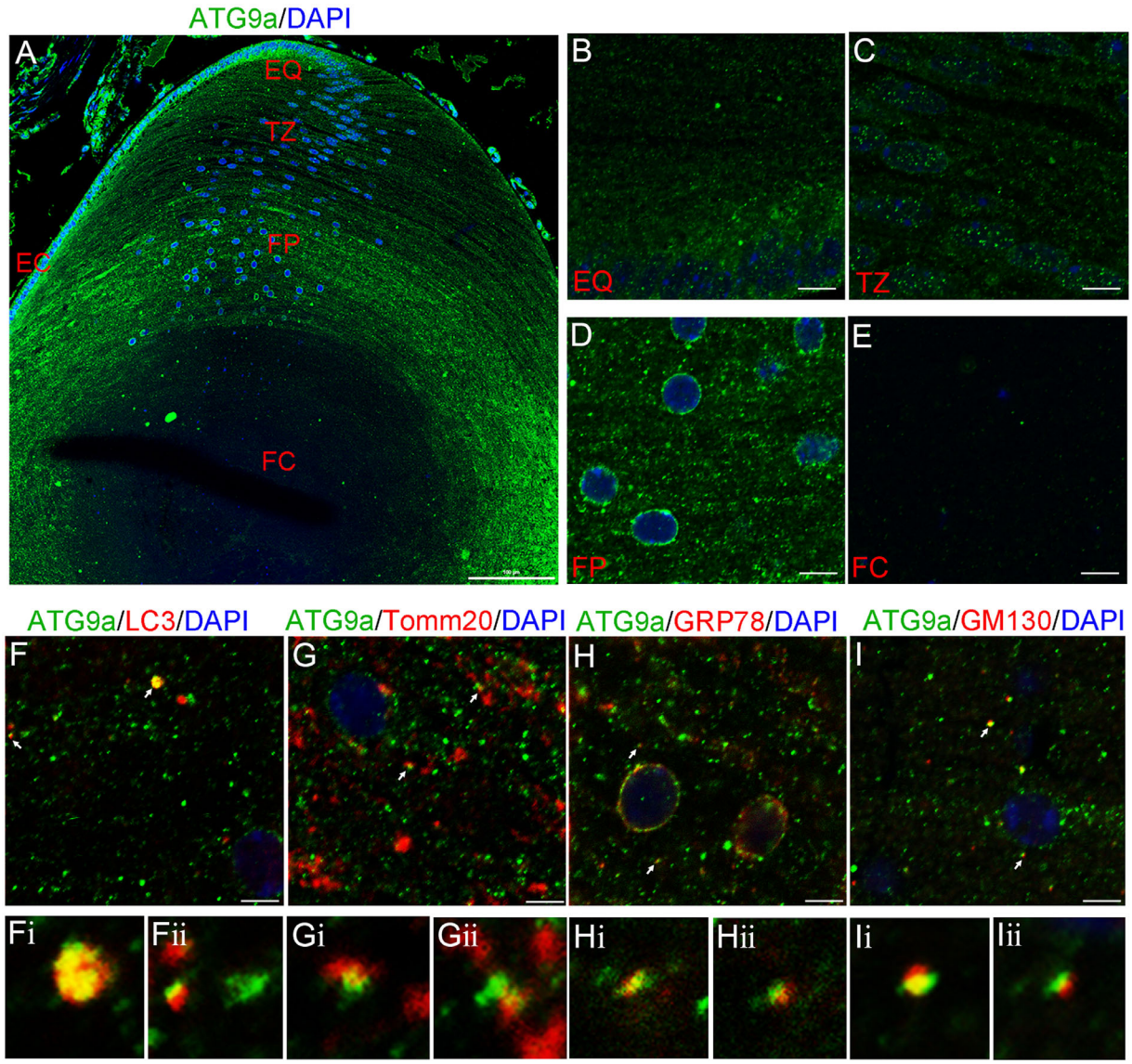

Figure 6. ATG9a is highly expressed in differentiating lens fibers. (**A**) The expression of ATG9a was analyzed by immunofluorescence in p7 WT mouse lenses. The nuclei were stained with DAPI. Bar, 100 µm. EC, central epithelium. EQ, equatorial epithelium. TZ, transition zone. FP, cortical fiber. FC, central fiber. (**B–E**) magnification of ATG9a expression in the EQ, TZ, FP, and FC in (**A**). *Bar:* 10 µm. (**F-F**ii) The colocalization between ATG9a and LC3 foci was observed in differentiating lens fibers. The nuclei were stained with DAPI. Bar, 5 µm. (**G–G**ii) The colocalization between ATG9a foci and Tomm20 was observed in differentiating lens fibers. The nuclei were stained with DAPI. *Bar:* 5 µm. (**H–H**ii) The colocalization between ATG9a foci and GRP78 was observed in differentiating lens fibers. The nuclei were stained with DAPI. Bar, 5 µm. (**I–I**ii) The colocalization between ATG9a foci and GM130 was observed in differentiating lens fibers. The nuclei were stained with DAPI. *Bar:* 5 µm.

lenses when treated with rapamycin for 12 hours ex vivo (Figs. 7I, 7J). Although HSF4 deficiency led to defective transcription of ATG9a, our results support the idea that the turnover of ATG9a protein by rapamycin treatment may have facilitated autophagy-mediated organelle degradation in HSF4^{del42} lenses.

Discussion

Mutations in HSF4 lead to congenital cataracts in humans.[35] In our previous studies, we found that knockout of HSF4 resulted in organelle degradation defects in lens fiber cells.[38] HSF4 transcriptionally activates lens specific DNases (e.g., DNase2β in humans and mice, and DNase1l1l in zebrafish) to promote the denucleation process during lens fiber terminal differentiation.[9,41] However, the mechanism by which HSF4 governs the degradation of other organelles is still unclear. In our present study, we find that HSF4 transcriptionally activates autophagy during lens differentiation, and activation of autophagy facilitates the organelle degradation in HSF4^{del42} lens fibers. There are some controversies regarding the roles of autophagy in the organelle removal of lens fibers. Morishita et al. found that knockout of ATG5 and VPS34 in mouse lenses did not affect the formation of the OFZ, although cataracts were indeed induced.[25] Those authors concluded that the organelle degradation of lens fibers occurs in an autophagy-independent manner. Subsequent studies have indicated that autophagy can also

Investigative Ophthalmology & Visual Science

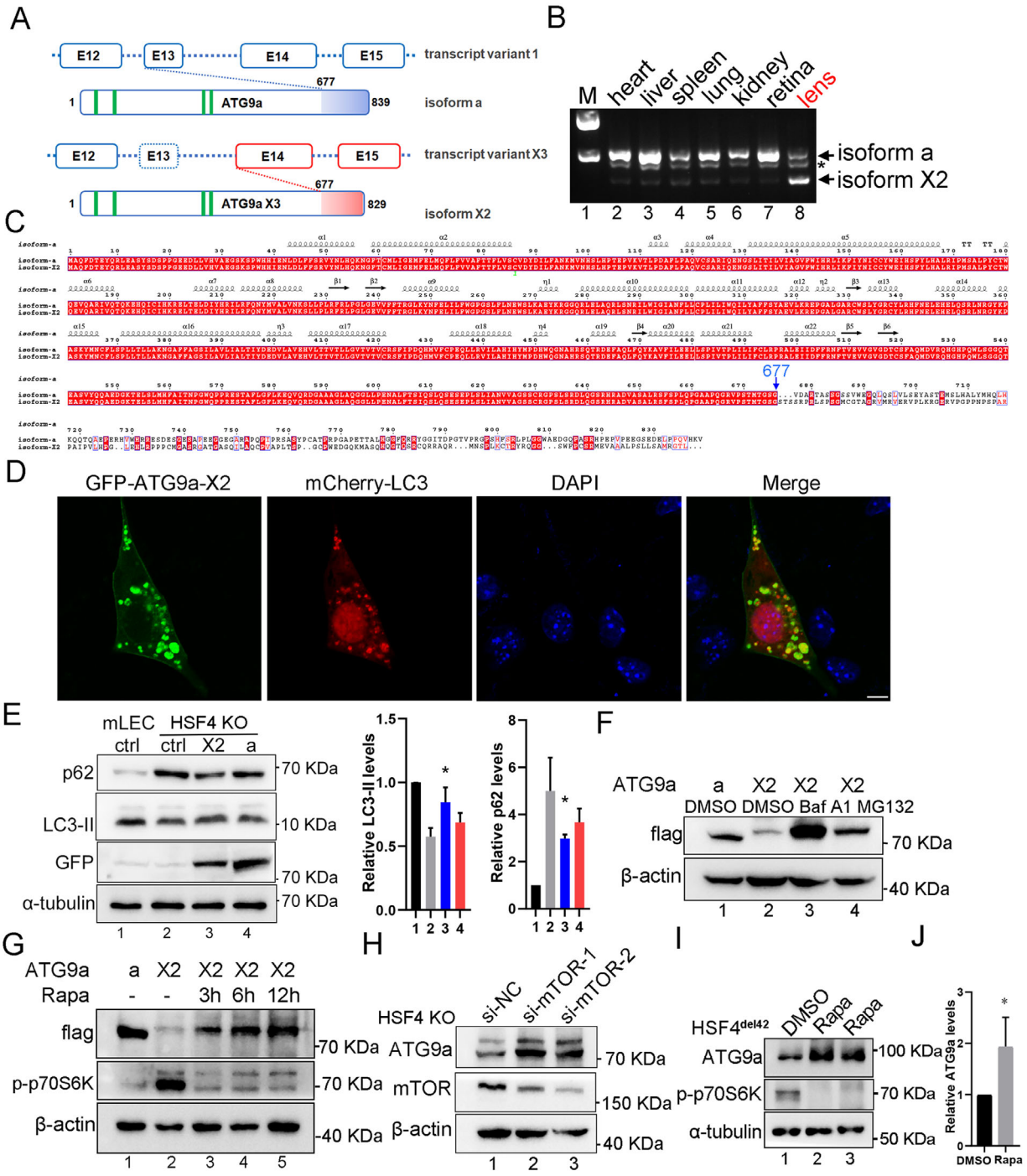

Figure 7. Rapamycin treatment elevated lens dominant ATG9a isoform levels. (**A**) Diagram of the canonical ATG9a isoform a and the lens-dominant isoform X2. (**B**) The expression of ATG9a isoforms a and X2 was detected by RT–PCR in various mouse tissues. M, marker. The *asterisk* indicated a nonspecific band. (**C**) The amino acid alignment between mouse ATG9a-a and X2 isoform. Strictly conserved positions were labeled with red background. The blue arrow indicated the position where the frameshift starts. (**D**)The colocalization between ATG9a-X2 and LC3 foci was analyzed in mLECs treated with 200 nM Baf-A1 for 6 hours. The nuclei were stained with DAPI. *Bar:* 5 µm. (**E**) the p62 and LC3-II levels were detected in WT and HSF4 KO mLECs that overexpressed GFP tagged ATG9a isoform a and X2. The levels of α-tubulin were used as controls. Student's t test was used for statistical analysis. n = 3, $^*P < 0.05$. (**F**) Protein levels of ATG9a-X2 were detected in mLEC cells treated with 200 nM Baf-A1 and 5 µM MG132 for six hours. The β-actin levels were as control. (**G**) Protein levels of ATG9a-X2 were detected in mLECs treated with 500 nM rapamycin for 3, 6 and 12 hours. The levels of phosphorylated p70S6K indicated the effects of rapamycin treatment. (**H**) Protein levels of ATG9a were detected in HSF4 KO mLECs, which mTOR was knocked down with siRNAs. The β-actin levels were used as controls. (**I, J**) Protein levels of ATG9a were detected in HSF4^{del42} lenses treated with 10 µM rapamycin for 12 hours ex vivo. The α-tubulin levels were used as controls. Student's *t* test was used for statistical analysis. n = 3, $^*P < 0.05$.

be accomplished independently of ATG5 and VPS34.[48,49] ATG5-independent alternative autophagy is required for the clearance of mitochondria during erythroid maturation and iPSC reprogramming.[50,51] These data suggested that alternative (ATG5- and VPS34- independent) autophagy may also contribute to organelle clearance during terminal differentiation of lens fibers. In a recent study, Morishita et al.[52] found that PLAAT phospholipases (PLAAT1 in zebrafish and PLAAT3 in mouse) translocated from the cytosol to organelles and destructed organelle membrane, and then caused organelle degradation during lens fiber differentiation. HSF4 is required for both the initial organelle membrane damage and then the following induced translocation of PLAATs.[52] Selective autophagy is required for degradation of intracellular organelles. It is interesting to investigate whether and how HSF4-controlled autophagy is involved in PLAATs-mediated organelle degradation. The organelle localization of ATG9a was similar with PLAAT3 in mouse differentiating lens fibers (Figs. 6G–I).[52] So, the roles of ATG9a in PLAAT3 translocation and thus organelle membrane damage require further study.

Our data indicated that rapamycin treatment also ameliorated organelle degradation defects in HSF4^{del42} lenses. Previous studies have shown that yeast ATG9 is degraded via the proteasome and that ATG9 turnover is impeded by rapamycin treatment.[47] We also found that rapamycin treatment stabilized the lens-dominant ATG9a isoform in lens epithelial cells and HSF4^{del42} lenses. ATG9a is the sole transmembrane protein among the core autophagy proteins. Our data showed that ATG9a is highly expressed and colocalizes with cellular organelles in differentiating lens fibers (Fig. 6). By interacting with the mitophagy receptor OPTN, ATG9a initiates the synthesis of autophagic membranes near ubiquitin-coated damaged mitochondria and promotes mitophagy.[53] ATG9A is ubiquitinated and then cooperates with GRASP55 to mediate Golgi fragmentation under heat stress.[54] With respect to the essential roles of ATG9a in macroautophagy and organelle-related selective autophagy, the stabilization of ATG9a by rapamycin treatment may at least partially contributes to the alleviation of OFZ defects in lenses. In addition, a recent study associated ATG9a mutations with immune dysregulation and hyperplasia in a patient exhibiting increased proliferation of T and B cells in lungs and brain and defects in lymphocyte memory cell populations after infection with Epstein-Barr virus.[55] Rapamycin treatment reduced the proliferation of the patient's cell and successfully cured the symptoms in the lungs and brain.[55] These data support the idea that rapamycin treatment could be an effective strategy for ATG9a-related disorders, including congenital cataracts.

It is still puzzling why and how ATG9a isoform X2 is particularly highly expressed in ocular lenses rather than other tissues. Compared with ATG9a isoform a, ATG9a-X2 has a distinct C-terminus produced by alternative splicing of exon 13. Although it has fewer amino acid residues, ATG9a-X2 was observed to have a higher molecular weight than ATG9a-a via immunoblotting (Figs. 7E–G). Our immunofluorescence data indicated that ATG9a-X2 formed more and larger LC3-positive foci than the ATG9a-a isoform in lens epithelial cells treated with the lysosome inhibitor Baf-A1 (Fig. 7D, Supplementary Fig. S6). These data hint that ATG9a-X2 may undergo posttranslational modifications, such as lipidation, to facilitate ATG9a association with autophagic vesicles. Another mystery exists regarding how rapamycin restored the ATG9a-X2 protein levels. Hu et al. demonstrated that degradation of the yeast ATG9a protein is regulated by the proteasomal pathway and can be impeded by rapamycin treatment. However, no essential ubiquitin-conjugating enzyme (E2 and E3 ligases) or ATG9a protein domain was identified for ATG9a degradation.[47] These data imply the existence of an intricate mechanism for ATG9a degradation. Zhang et al.[56] showed that mTORC1 activation promotes protein degradation by elevating intact and active proteasome levels. Whether ATG9a turnover by rapamycin treatment depends on the regulation of proteasome levels requires further investigation. We speculate that a more efficient ATG9a isoform is required for the fast and dramatic formation of the OFZ during lens fiber terminal differentiation, although more evidence is needed.

In conclusion, HSF4^{del42} mice displayed defects in organelle removal and autophagic degradation function in lens fibers. Activation of autophagy ex vivo and in vivo accelerated the degradation of nonnuclear organelles in HSF4^{del42} mouse lenses. HSF4 facilitated autophagosome biogenesis and maturation, and transcriptionally regulated ATG9a expression. The lens-dominant ATG9a isoform had vulnerable protein stability, and rapamycin treatment increased the levels of ATG9a in HSF4-deficient lenses. Our data indicate the essential role of ATG9a-related autophagy in HSF4 mediated lens differentiation and shed light on therapies for congenital cataracts.

Acknowledgments

The authors thank Mingli Wang, Hui Li, and Jing Li for technical support.

Supported by National Natural Science Foundation of China (32070585, 81900889 and 81770911) and Henan Natural Science Funds for Excellent Young Scholar (212300410025).

Disclosure: **J. Zhang**, None; **N. Jiang**, None; **C. Du**, None; **H. Guo**, None; **R. Meng**, None; **X. Hou**, None; **M. Liu**, None; **Y. Hu**, None; **X. Cui**, None

References

1. Cvekl A, Ashery-Padan R. The cellular and molecular mechanisms of vertebrate lens development. *Development*. 2014;141:4432–4447.
2. Wride MA. Cellular and molecular features of lens differentiation: a review of recent advances. *Differentiation*. 1996;61:77–93.
3. Cvekl A, McGreal R, Liu W. Lens development and crystallin gene expression. *Prog Mol Biol Transl Sci*. 2015;134:129–167.
4. McAvoy JW, Chamberlain CG, de Iongh RU, Hales AM, Lovicu FJ. Lens development. *Eye (Lond)*. 1999;13(Pt 3b):425–437.
5. Brennan L, Disatham J, Kantorow M. Mechanisms of organelle elimination for lens development and differentiation. *Exp Eye Res*. 2021;209:108682.
6. Wride MA. Lens fibre cell differentiation and organelle loss: many paths lead to clarity. *Philos Trans R Soc Lond B Biol Sci*. 2011;366:1219–1233.
7. Li J, Chen X, Yan Y, Yao K. Molecular genetics of congenital cataracts. *Exp Eye Res*. 2020;191:107872.
8. Nishimoto S, Kawane K, Watanabe-Fukunaga R, et al. Nuclear cataract caused by a lack of DNA degradation in the mouse eye lens. *Nature*. 2003;424:1071–1074.
9. Zhang J, Cui WW, Du C, et al. Knockout of DNase1l1l abrogates lens denucleation process and causes cataract

in zebrafish. *Biochim Biophys Acta Mol Basis Dis*. 2020; 1866:165724.
10. Yu L, Chen Y, Tooze SA. Autophagy pathway: cellular and molecular mechanisms. *Autophagy*. 2018;14:207–215.
11. Gatica D, Lahiri V, Klionsky DJ. Cargo recognition and degradation by selective autophagy. *Nat Cell Biol*. 2018;20:233–242.
12. Chen J, Ma Z, Jiao X, et al. Mutations in FYCO1 cause autosomal-recessive congenital cataracts. *Am J Hum Genet*. 2011;88:827–838.
13. Khan SY, Ali M, Kabir F, et al. The role of FYCO1-dependent autophagy in lens fiber cell differentiation. *Autophagy*. 2022;18:2198–2215.
14. Nieto-Torres JL, Shanahan SL, Chassefeyre R, et al. LC3B phosphorylation regulates FYCO1 binding and directional transport of autophagosomes. *Curr Biol*. 2021;31:3440–3449.
15. Wang Z, Miao G, Xue X, et al. The Vici syndrome protein EPG5 is a Rab7 effector that determines the fusion specificity of autophagosomes with late endosomes/lysosomes. *Mol Cell*. 2016;63:781–795.
16. Cullup T, Kho AL, Dionisi-Vici C, et al. Recessive mutations in EPG5 cause Vici syndrome, a multisystem disorder with defective autophagy. *Nat Genet*. 2013;45:83–87.
17. Byrne S, Jansen L, U-King-Im JM, et al. EPG5-related Vici syndrome: a paradigm of neurodevelopmental disorders with defective autophagy. *Brain*. 2016;139:765–781.
18. Aligianis IA, Johnson CA, Gissen P, et al. Mutations of the catalytic subunit of RAB3GAP cause Warburg micro syndrome. *Nat Genet*. 2005;37:221–223.
19. Borck G, Wunram H, Steiert A, et al. A homozygous RAB3GAP2 mutation causes Warburg micro syndrome. *Hum Genet*. 2011;129:45–50.
20. Liegel RP, Handley MT, Ronchetti A, et al. Loss-of-function mutations in TBC1D20 cause cataracts and male infertility in blind sterile mice and Warburg micro syndrome in humans. *Am J Hum Genet*. 2013;93:1001–1014.
21. Sidjanin DJ, Park AK, Ronchetti A, Martins J, Jackson WT. TBC1D20 mediates autophagy as a key regulator of autophagosome maturation. *Autophagy*. 2016;12:1759–1775.
22. Tu C, Li H, Liu X, et al. TDRD7 participates in lens development and spermiogenesis by mediating autophagosome maturation. *Autophagy*. 2021;17:3848–3864.
23. Spang N, Feldmann A, Huesmann H, et al. RAB3GAP1 and RAB3GAP2 modulate basal and rapamycin-induced autophagy. *Autophagy*. 2014;10:2297–2309.
24. Matsui M, Yamamoto A, Kuma A, Ohsumi Y, Mizushima N. Organelle degradation during the lens and erythroid differentiation is independent of autophagy. *Biochem Biophys Res Commun*. 2006;339:485–489.
25. Morishita H, Eguchi S, Kimura H, et al. Deletion of autophagy-related 5 (Atg5) and Pik3c3 genes in the lens causes cataract independent of programmed organelle degradation. *J Biol Chem*. 2013;288:11436–11447.
26. Costello MJ, Brennan LA, Basu S, et al. Autophagy and mitophagy participate in ocular lens organelle degradation. *Exp Eye Res*. 2013;116:141–150.
27. McWilliams TG, Prescott AR, Villarejo-Zori B, Ball G, Boya P, Ganley IG. A comparative map of macroautophagy and mitophagy in the vertebrate eye. *Autophagy*. 2019;15:1296–1308.
28. Basu S, Rajakaruna S, Reyes B, Van Bockstaele E, Menko AS. Suppression of MAPK/JNK-MTORC1 signaling leads to premature loss of organelles and nuclei by autophagy during terminal differentiation of lens fiber cells. *Autophagy*. 2014;10:1193–1211.
29. Gheyas R, Ortega-Alvarez R, Chauss D, Kantorow M, Menko AS. Suppression of PI3K signaling is linked to autophagy activation and the spatiotemporal induction of the lens organelle free zone. *Exp Cell Res*. 2022;412:113043.
30. Ping X, Liang J, Shi K, et al. Rapamycin relieves the cataract caused by ablation of Gja8b through stimulating autophagy in zebrafish. *Autophagy*. 2021;17:3323–3337.
31. Brennan LA, McGreal-Estrada R, Logan CM, Cvekl A, Menko AS, Kantorow M. BNIP3L/NIX is required for elimination of mitochondria, endoplasmic reticulum and Golgi apparatus during eye lens organelle-free zone formation. *Exp Eye Res*. 2018;174:173–184.
32. Lachke SA, Alkuraya FS, Kneeland SC, et al. Mutations in the RNA granule component TDRD7 cause cataract and glaucoma. *Science*. 2011;331:1571–1576.
33. Akerfelt M, Morimoto RI, Sistonen L. Heat shock factors: integrators of cell stress, development and lifespan. *Nat Rev Mol Cell Biol*. 2010;11:545–555.
34. Fujimoto M, Izu H, Seki K, et al. HSF4 is required for normal cell growth and differentiation during mouse lens development. *EMBO J*. 2004;23:4297–4306.
35. Ke T, Wang QK, Ji B, et al. Novel HSF4 mutation causes congenital total white cataract in a Chinese family. *Am J Ophthalmol*. 2006;142:298–303.
36. Smaoui N, Beltaief O, BenHamed S, et al. A homozygous splice mutation in the HSF4 gene is associated with an autosomal recessive congenital cataract. *Invest Ophthalmol Vis Sci*. 2004;45:2716–2721.
37. Bu L, Jin Y, Shi Y, et al. Mutant DNA-binding domain of HSF4 is associated with autosomal dominant lamellar and Marner cataract. *Nat Genet*. 2002;31:276–278.
38. Gao M, Huang Y, Wang L, et al. HSF4 regulates lens fiber cell differentiation by activating p53 and its downstream regulators. *Cell Death Dis*. 2017;8:e3082.
39. Liang L, Liegel R, Endres B, Ronchetti A, Chang B, Sidjanin DJ. Functional analysis of the Hsf4(lop11) allele responsible for cataracts in lop11 mice. *Mol Vis*. 2011;17:3062–3071.
40. Shi X, Cui B, Wang Z, et al. Removal of Hsf4 leads to cataract development in mice through down-regulation of gamma S-crystallin and Bfsp expression. *BMC Mol Biol*. 2009; 10:10.
41. Cui X, Wang L, Zhang J, et al. HSF4 regulates DLAD expression and promotes lens de-nucleation. *Biochim Biophys Acta*. 2013;1832:1167–1172.
42. Cui X, Du C, Wan S, et al. Deficiency of heat shock factor 4 promotes lens epithelial cell senescence through upregulating p21(cip1) expression. *Biochim Biophys Acta Mol Basis Dis*. 2021;1867:166233.
43. Cui X, Feng R, Wang J, et al. Heat shock factor 4 regulates lysosome activity by modulating the alphaB-crystallin-ATP6V1A-mTOR complex in ocular lens. *Biochim Biophys Acta Gen Subj*. 2020;1864:129496.
44. Hurley JH, Young LN. Mechanisms of Autophagy Initiation. *Annu Rev Biochem*. 2017;86:225–244.
45. Viret C, Faure M. Regulation of Syntaxin 17 during autophagosome maturation. *Trends Cell Biol*. 2019;29:1–3.
46. Chumpen RS, Gomez-Sanchez R, Verlhac P, et al. –Atg9 interactions via its transmembrane domains are required for phagophore expansion during autophagy [published online ahead of print November 10, 2022]. *Autophagy*, doi:10.1080/15548627.2022.2136340.
47. Hu G, Rios L, Yan Z, et al. Autophagy regulator Atg9 is degraded by the proteasome. *Biochem Biophys Res Commun*. 2020;522:254–258.
48. Nishida Y, Arakawa S, Fujitani K, et al. Discovery of Atg5/Atg7-independent alternative macroautophagy. *Nature*. 2009;461:654–658.
49. Zhou X, Wang L, Hasegawa H, et al. Deletion of PIK3C3/Vps34 in sensory neurons causes rapid neurodegeneration by disrupting the endosomal but not the

Investigative Ophthalmology & Visual Science

autophagic pathway. *Proc Natl Acad Sci USA*. 2010;107:9424–9429.

50. Ma T, Li J, Xu Y, et al. Atg5-independent autophagy regulates mitochondrial clearance and is essential for iPSC reprogramming. *Nat Cell Biol*. 2015;17:1379–1387.
51. Honda S, Arakawa S, Nishida Y, Yamaguchi H, Ishii E, Shimizu S. Ulk1-mediated Atg5-independent macroautophagy mediates elimination of mitochondria from embryonic reticulocytes. *Nat Commun*. 2014;5:4004.
52. Morishita H, Eguchi T, Tsukamoto S, et al. Organelle degradation in the lens by PLAAT phospholipases. *Nature*. 2021;592:634–638.
53. Yamano K, Kikuchi R, Kojima W, et al. Critical role of mitochondrial ubiquitination and the OPTN-ATG9A axis in mitophagy. *J Cell Biol*. 2020;219(9):e201912144.
54. Luo Q, Liu Q, Cheng H, et al. Nondegradable ubiquitinated ATG9A organizes Golgi integrity and dynamics upon stresses. *Cell Rep*. 2022;40:111195.
55. Hu G, Hauk PJ, Zhang N, et al. Autophagy-associated immune dysregulation and hyperplasia in a patient with compound heterozygous mutations in ATG9A. *Autophagy*. 2023;19:678–691.
56. Zhang Y, Nicholatos J, Dreier JR, et al. Coordinated regulation of protein synthesis and degradation by mTORC1. *Nature*. 2014;513:440–443.